

THE THERMAL BEHAVIOUR OF BTAW, A HIGH NITROGEN FUEL

D. E. G. Jones*, K. Armstrong, T. Parekunnel and Q. S. M. Kwok

Canadian Explosives Research Laboratory, Natural Resources Canada, 555 Booth Street, Ottawa, ON, K1A 0G1, Canada

BTAW (*bis*-(1(2)H-tetrazol-5yl)-amine monohydrate) has recently been considered for use as a low-smoke pyrotechnic fuel. There is relatively little information available in the literature concerning the thermal properties of BTAW or its precursors. In the present work, various thermoanalytical experiments were performed on BTAW and BTA (*bis*-(1(2)H-tetrazol-5yl)-amine) in an effort to better characterize the thermal stability and decomposition of these compounds.

Variable heating rate studies were carried out on BTAW samples in a helium atmosphere using DSC and TG. Two steps were seen in the results: dehydration followed by decomposition. Kinetic parameters were determined for both of these steps using a number of methods. Experiments using simultaneous TG-DTA coupled with FTIR and MS were performed on BTAW in both helium and dry and CO₂ free air atmospheres, and evolved gas analysis was used to determine the gaseous decomposition products. The thermal stability of BTAW and BTA was examined using accelerating rate calorimetry (ARC).

Keywords: *pyrotechnic fuel, thermal stability of BTA and BTAW*

Introduction

Typically, pyrotechnic formulations consist of carbonaceous fuels with metal salts added to oxidize the fuel and colour the flame. These combinations tend to produce an abundance of noxious smoke and ash, the result of partial combustion, and the generation of non-gaseous products, particularly metal oxides. Chlorinated polymers were introduced for colour enhancement but they still produce large amounts of smoke. High-nitrogen compounds were also introduced with more success. Chavez and Hiskey have reported work on 3,6-dihydrazino-*s*-tetrazine (DHT) in which it was mixed with non-metallic oxidizers and 5 mass% coloring agents, resulting in the production of little smoke and ash [1].

Other high-nitrogen compounds studied for use as low smoke pyrotechnic fuels are BTAW (*bis*-(1(2)H-tetrazol-5yl)-amine monohydrate), shown in Fig. 1, and 5,5'-*bis*-1H-tetrazole (BT).

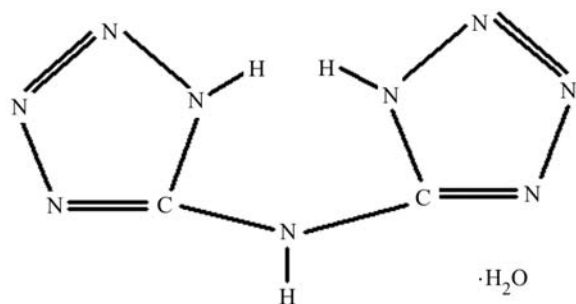


Fig. 1 Structure for BTAW

These compounds are diprotic acids that react with basic amines to form mono- and di-aminated salts, and react with metal carbonates or hydroxides to form metal salts. Chavez *et al.* have recently reported that, by preparing BTAW and BT with different ratios and compositions, it is possible to achieve greater control and variability in burn rate and ignitability of high-nitrogen pyrotechnic formulations than with DHT alone [2]. Various characteristics of these two molecules, their hydrates and salts, were examined by Chavez, including impact sensitivity, thermal behaviour by TG as well as the dehydration of BTAW to BTA (*bis*-(1(2)H-tetrazol-5yl)-amine) [2]. It was noted that BTA exhibited greater impact sensitivity than the hydrated form, BTAW. Nedelko *et al.* studied the kinetics and decomposition products of BTA using thermogravimetry, volumetry, calorimetry, IR-spectroscopy and mass spectroscopy [3].

The present paper includes a detailed description of the current work on BTAW. Two variable heating rate studies on BTAW, one using DSC and the other using TG, a study of the thermal decomposition using simultaneous TG-DTA coupled with FTIR and MS, and an investigation of the thermal stability of BTAW and BTA in air and argon atmospheres using accelerating rate calorimetry (ARC) are described in this paper.

Experimental

Samples of BTAW containing 20% water were used as starting materials. These as-received samples were

* Author for correspondence: djones@nrca.gc.ca

used in the DSC heating rate study. Two methods were used to pre-dry the BTaw. One method involved drying the BTaw in situ, i.e. in the ARC studies, for 3 h at 120°C in an open system. The other method consisted of drying BTaw in an oven at 50 or 120°C for several hours. BTaw sample with no excess water was obtained by drying at 50°C, whereas BTA was generated by removing water of hydration at 120°C. The pre-dried sample at 50°C was used in the TG and TG-DTA-FTIR-MS studies. Samples obtained from both methods were used in the ARC studies.

A TA Instrument (TAI) 2910 DSC was used for a variable heating rate study of BTaw following ASTM standard test method E 698-01 [4]. Hermetic pin-hole Al pans (75 μm hole) containing about 0.25 mg of BTaw were heated from 30 to 350°C at the rates of 0.5, 1, 2, 5, 8 and 10°C min⁻¹. The DSC was calibrated for heat flow [5] and temperature [6]. An empty pan was used as the reference.

TG studies on BTaw were conducted using two different modules: the TAI 2950 and the TAI Q500. The consistency of results between both modules was verified by performing repeat measurements at the same heating rate. Sample sizes of 1 mg were placed in aluminum pans. The system was purged with helium at a flow rate of 100 mL min⁻¹, split 60:40 between the furnace and the balance. The samples were heated from 30 to 350°C at rates of 1, 2, 5 and 10°C min⁻¹. TG instruments were calibrated for mass using the procedures recommended by the manufacturer and for temperature using the Curie point method as described in ASTM method E1582 [7].

Details of the instruments used to obtain simultaneous TG-DTA-FTIR-MS data can be found in an earlier publication [8]. The TG-DTA-FTIR-MS data were acquired simultaneously to study the thermal behaviour of BTaw and to identify the gases that evolved while the BTaw sample was heated. Samples and reference (Pt foil) of 5 mg were heated in alumina pans at a rate of 5°C min⁻¹. Samples were purged in helium and in air at rates of 100 and 50 mL min⁻¹, respectively. The acquisition rate of the FTIR was two and one scans every minute for helium and air, respectively. Data were acquired using bargraph scan, from 5 to 100 amu (atomic mass unit) at a speed of 0.2 s amu⁻¹. The MS was calibrated for mass alignment and amplifier signal.

The ARC measurements were performed using two instruments: one adiabatic calorimeter was distributed by TIAX LLC (formerly known as Arthur D. Little Inc.) while the other was a Thermal Hazard Technology (THT) instrument. Samples of about 0.5 g were placed in lightweight spherical titanium vessels. The ARC experiments were started at an ambient pressure of either air or argon. The stan-

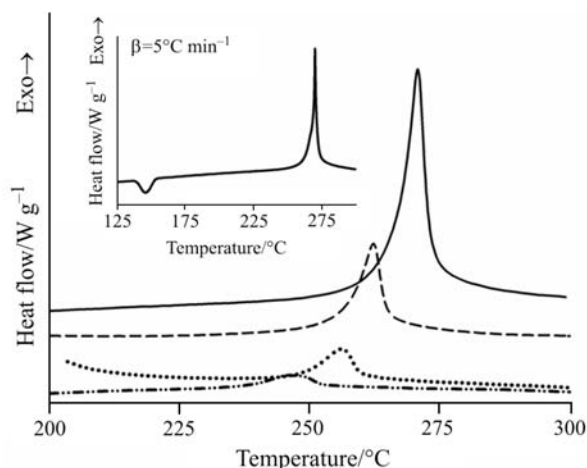


Fig. 2 DSC curves for BTaw at — 5°C min⁻¹, --- 2°C min⁻¹, ··· 1°C min⁻¹ and - · - · 0.5°C min⁻¹

dard ARC procedure of ‘heat-wait-search’ (HWS) was used [9, 10] with a 5°C heat step.

Results and discussion

Dehydration

DSC results

Typical thermal curves of BTaw obtained at various heating rates are shown in Fig. 2. The inset shows the entire range of the thermal curve obtained at 5°C min⁻¹, including an endotherm in the 125 to 150°C range, which is attributed to the dehydration of BTaw. The average enthalpy of dehydration is 268±15 J g⁻¹ or 43±2 kJ (mol BTaw)⁻¹. Hydrogen bonding energies for formic acid are 20 kJ mol⁻¹ [11]. Thus, the result for BTaw suggests that there is strong hydrogen bonding between the water and BTA molecules.

Kinetic parameters for the dehydration step were determined from a series of variable heating rate ex-

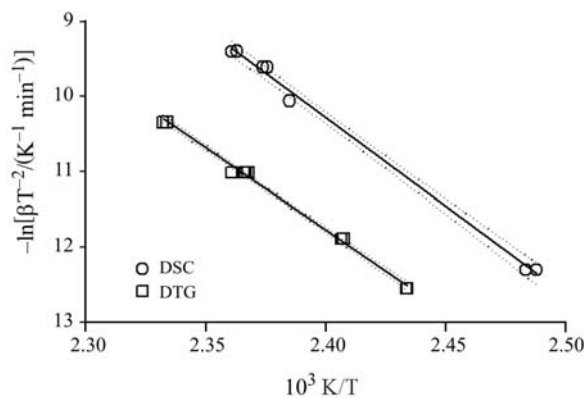


Fig. 3 Plot of $-\ln[\beta T^{-2}/(\text{K}^{-1} \text{min}^{-1})]$ vs. $10^3 \text{ K}/T$ for the dehydration step using data from DTG and DSC. ··· 95% confidence limits

periments following the ASTM method E698 [4]. The results were determined from Fig. 3, which is a plot of $-\ln[\beta T^{-2}/(K^{-1} \text{ min}^{-1})]$ vs. $10^3 K/T$ for the peak temperatures (T) of the dehydration endotherm at different heating rates (β). The activation energy, E , was found to be $197 \pm 5 \text{ kJ mol}^{-1}$, indicating that the water molecule is strongly bound to BTA. Using this value of E in conjunction with the calculated pre-exponential factor, $\ln(Z/\text{min}^{-1}) = 46 \pm 1$, the rate constant was determined to be $\ln[k(144^\circ\text{C})/\text{min}^{-1}] = -11 \pm 2$.

TG results

A two-step mass loss was observed in all experiments, the first step represents dehydration and the second step is a result of decomposition. Figure 4 shows a typical TG curve obtained from the variable heating rate study. An initial 9–10% mass loss was observed in the 130–160°C range. This corresponds to the loss of 1 mol of H_2O from 1 mol of BTAW, for which the calculated mol% H_2O is 10.5.

In a study by Chavez *et al.* [2], it was reported that hydrated water in a BTAW sample was lost from 74 to 116°C. In this particular study the heating rate used during the TG experiment was $0.1^\circ\text{C min}^{-1}$, which is substantially lower than the heating rates used in the present work. Thus, the loss of hydrated water at lower temperatures was expected because of the much slower heating rate.

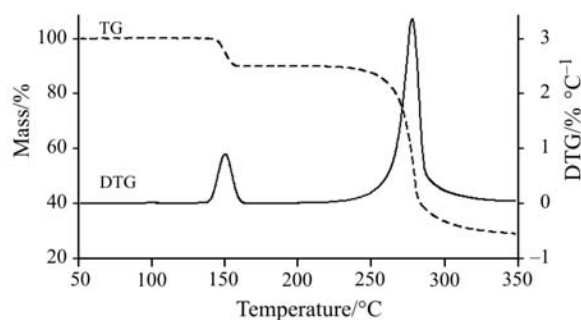


Fig. 4 TG and DTG curves for BTAW for $\beta = 5^\circ\text{C min}^{-1}$

Kinetic parameters, $E/(\text{kJ mol}^{-1})$ and $\ln(Z/\text{min}^{-1})$, were obtained for the dehydration step using ASTM method E 1641 [12], which is based on the assumption that the dehydration obeys first-order kinetics. As recommended by the ASTM method, calculations were carried out at several different levels of conversion: 5, 10, 15 and 20%. The results can be seen in Fig. 5, which is a plot of $\ln\beta$ vs. $10^3 K/T$, where T is the temperature of these different conversion levels, α , obtained at various heating rates (β). Table 1 shows that the values of E do not vary between the range of conversion level examined and an average value of $193 \pm 5 \text{ kJ mol}^{-1}$ was determined. This result is in good agreement with the DSC results in this study, as seen from Fig. 3. An average value of the pre-exponential factor was also calculated, giving $\ln(Z/\text{min}^{-1}) = 57 \pm 2$.

With the peak temperatures from the DTG data, ASTM method E698 [4] was employed as another technique to determine kinetic parameters. The results are shown in Fig. 3. Calculations of the kinetic parameters yielded $E = 182 \pm 4 \text{ kJ mol}^{-1}$ and $\ln(Z/\text{min}^{-1}) = 41 \pm 1$.

Using the calculated kinetic parameters, E and $\ln Z$, previously mentioned, the values for $\ln k$ were cal-

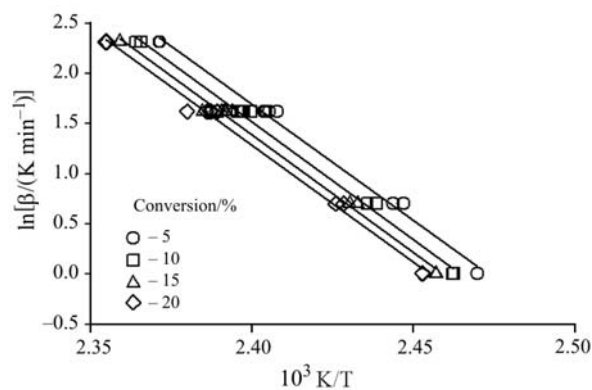


Fig. 5 Plot of $\ln(\beta/\text{K min}^{-1})$ vs. $10^3 K/T$ for the dehydration step with various heating rates

Table 1 Comparison of kinetic parameters from the variable heating rate studies

Method	Conversion/%	Dehydration			Decomposition		
		$E/(\text{kJ mol}^{-1})$	$\ln(Z/\text{min}^{-1})$	$\ln(k/\text{min}^{-1})^a$	$E/(\text{kJ mol}^{-1})$	$\ln(Z/\text{min}^{-1})$	$\ln(k/\text{min}^{-1})^b$
DSC ASTM E698	–	197 ± 5	46 ± 1	-11 ± 2	222 ± 16	38 ± 4	-12 ± 6
	–	182 ± 4	41 ± 1	-11 ± 1	236 ± 5	41 ± 1	-12 ± 1
	–	178 ± 3	–	-1 ± 1	–	–	–
TG ASTM E1641	5	192 ± 6	57 ± 2	2 ± 3	180 ± 6	43 ± 1	–
	10	194 ± 5	57 ± 2	1 ± 3	197 ± 9	46 ± 3	2 ± 3
	15	194 ± 5	57 ± 1	1 ± 2	203 ± 10	47 ± 2	2 ± 3
	20	193 ± 5	57 ± 1	1 ± 2	209 ± 8	48 ± 2	1 ± 3

^acalculated at 144°C , ^bcalculated at 265°C

culated for the dehydration step at a common temperature of 144°C in order to compare the results obtained by ASTM E698 and ASTM E1641. The value for the DTG data was $\ln(k/\text{min}^{-1}) = -11 \pm 1$, which is in agreement with the value calculated from the DSC data. From the TG data, an average was taken of the rate constants and found to be $\ln(k/\text{min}^{-1}) = 1 \pm 2$, which is significantly higher than those found using the DSC and DTG data. This was expected given the difference in pre-exponential factors. This difference could be due to the fact that the values calculated using the TG data were obtained in the early stages of the dehydration in comparison with the values from the DSC and DTG data, which were obtained at much later stages.

The software IsoKin [13] was then used to perform a model free kinetic (MFK) analysis on the first mass loss from the TG results. The model-free approach makes use of an isoconversional method that allows for evaluating a dependence of the effective activation energy on the extent of conversion [14]. These results can be found in Fig. 6, which shows the dependence of the activation energy on the extent of reaction. The MFK results show that the activation energy remains consistent throughout the extent of the dehydration step, indicating a single-stage process, with a mean value of $178 \pm 3 \text{ kJ mol}^{-1}$ for $0.1 < \alpha < 0.8$. From the MFK analysis, the mean value of $\ln[f(\alpha)Z/\text{min}^{-1}]$ is 49.7 ± 0.8 , where $f(\alpha)$ is the reaction model.

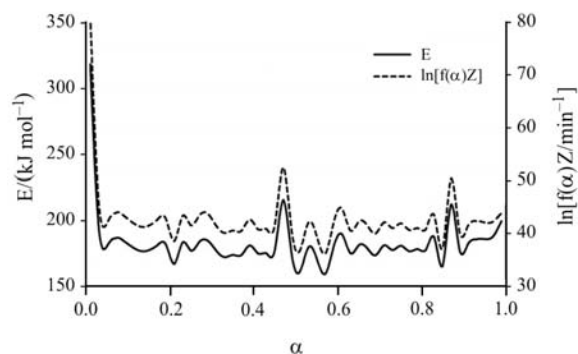


Fig. 6 BTaw (pre-dried at 50°C) IsoKin TG dehydration results ($\beta = 1$ to $10^\circ\text{C min}^{-1}$)

Decomposition

DSC results

The results of the heating rate study, using ASTM method E698 [4], on the decomposition of BTaw are shown in Fig. 7, which is a plot of $-\ln[\beta T^{-2}/(\text{K}^{-1} \text{min}^{-1})]$ vs. $10^3 \text{ K}/T$. This plot was used to determine the values of the kinetic parameters, E and $\ln(Z/\text{min}^{-1})$, for BTaw. Only results from the 0.5, 1, 2 and 5°C min^{-1} heating rates were included as the heat generated for the 8 and $10^\circ\text{C min}^{-1}$ runs exceeded the maximum heat generation limit of 8 mW recom-

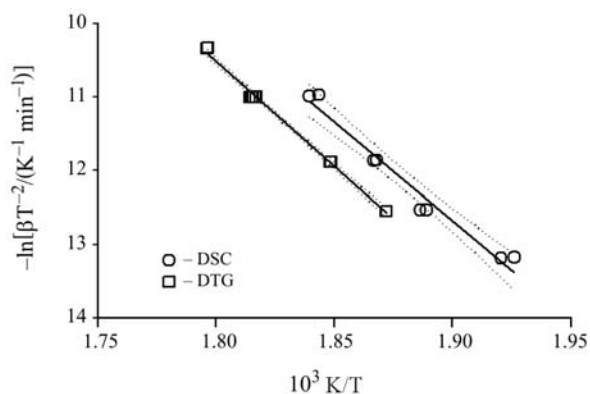


Fig. 7 Plot of $-\ln[\beta T^{-2}/(\text{K}^{-1} \text{min}^{-1})]$ vs. $10^3 \text{ K}/T$ for the thermal decomposition step using data from DTG and DSC. . . . 95% confidence limits

mended in the ASTM method E968 [5]. The kinetic parameters determined are $E = 222 \pm 16 \text{ kJ mol}^{-1}$ and $\ln(Z/\text{min}^{-1}) = 38 \pm 4$. A $\ln(k/\text{min}^{-1})$ value of -12 ± 6 was calculated at 265°C .

To confirm the kinetic results, a sample of BTaw was aged at 234°C for 64 min, the calculated half-life of BTaw at this temperature from analysis of the data, and then immediately quenched to a temperature at least 50°C lower. This aged sample was then heated at 5°C min^{-1} and its thermal curve recorded. The peak area for this curve was $737 \pm 5 \text{ J g}^{-1}$. When compared to $1.48 \pm 0.01 \text{ kJ g}^{-1}$, the peak area for the unaged sample of BTaw run at the same heating rate, it is seen that the peak area of the aged sample shows good agreement with the predicted value. Thus, the values determined for the kinetic parameters are good estimates for BTaw. The DSC thermal curves for the aged and unaged samples of BTaw are shown in Fig. 8.

Using the data collected from the DSC, a MFK analysis was performed with the IsoKin software package [13]. The results for E and $\ln[f(\alpha)Z/\text{min}^{-1}]$

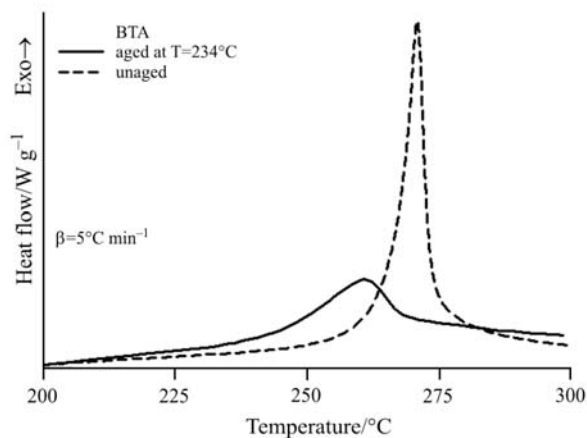


Fig. 8 Comparison of the DSC thermal curve of an aged BTA sample with that of an unaged sample

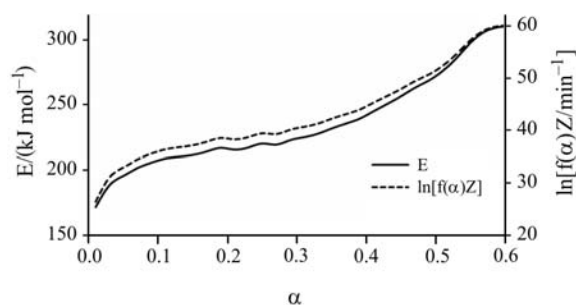


Fig. 9 BTAw IsoKin DSC results for $\beta=0.5$ to 5°C min^{-1}

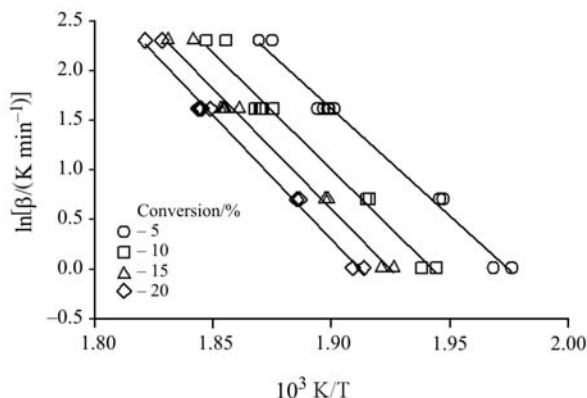


Fig. 10 Plot of $\ln(\beta/\text{K min}^{-1})$ vs. 10^3 K/T for the thermal decomposition step with various heating rates

are shown in Fig. 9. E has increasing values as the extent of conversion, α , increases to 0.6. This observation suggests that parallel reactions are occurring from $0.1 < \alpha < 0.6$.

TG results

The second observed mass loss corresponds to thermal decomposition. This step occurred with a mass loss of approximately 60% in the $250\text{--}290^\circ\text{C}$ range, as shown in Fig. 4. When using ASTM method E1641 [11] to evaluate kinetic parameters for the decomposition step, the calculated values for E and $\ln(Z)$ were observed to increase as the extent of conversion increased (Table 1 and Fig. 10).

Decomposition of BTAW was reported [2] to commence at approximately 175°C using a heating rate of $0.1^\circ\text{C min}^{-1}$. With a heating rate significantly lower than those used in this study, it was expected that the onset temperature in the literature work would also be lower due to the dependence of the onset temperature on the heating rate.

Nedelko *et al.* reported [3] kinetic parameters corresponding to both first order decomposition and a first order catalytic reaction. For the first order decomposition of BTAW, kinetic parameters of $E=197\pm 5 \text{ kJ mol}^{-1}$ and $\ln(Z/\text{min}^{-1})=40\pm 5$ were given.

A value for $\ln k = -6\pm 5$ was calculated from this data at 242°C . In order to compare this value with the rate constants from this study, values for $\ln k$ were also calculated at 242°C . From the TG data at 5% conversion, it was found that $\ln(k/\text{min}^{-1})=1\pm 2$, and at 10% conversion, $\ln(k/\text{min}^{-1})=0\pm 3$. These values agree with the results from Nedelko within the margin of error. From the DSC data, a value of $\ln(k/\text{min}^{-1})=-14\pm 5$ was found. This value was also within the margin of error in comparison with Nedelko's results; however, using data from the DTG results to calculate the rate constant gave $\ln(k/\text{min}^{-1})=-14\pm 2$, which did not fall within the range of error.

Using the DTG peak temperatures and ASTM method E698 [4], kinetic parameters of $E=236\pm 5 \text{ kJ mol}^{-1}$ and $\ln(Z/\text{min}^{-1})=41\pm 1$ were calculated (Fig. 7). Both of these values are consistent with those obtained from the DSC heating rate study and provide a good estimate of the kinetic parameters for BTAW. Values for $\ln(k/\text{min}^{-1})$ were calculated using a common temperature of 265°C . The DTG $\ln k$ value was found to be $-12\pm 1 \text{ min}^{-1}$ while the TG value at 10% conversion was $2\pm 3 \text{ min}^{-1}$. This difference was not unexpected as the results from ASTM method E1641 (Fig. 10) showed that the kinetic parameters vary with extent of conversion. The DTG value for $\ln k$ was consistent, however, with that obtained from the DSC results.

The MFK results for this second step, seen in Fig. 11, revealed that E slowly increases for $\alpha < 0.6$. In this range, MFK analysis also showed that the values of $\ln[f(\alpha)Z/\text{min}^{-1}]$ slowly increased from about 30 to 50. The variation of E with α is consistent with the results obtained using ASTM method E1641 (Fig. 10). As in the DSC decomposition results, this dependence of E on α and its increasing nature suggest that parallel reactions are occurring in the range up to $\alpha < 0.6$.

TG-DTA-FTIR-MS results

The thermal decomposition of BTAW was also studied using TG-DTA-FTIR-MS. A TG-DTA-FTIR-MS

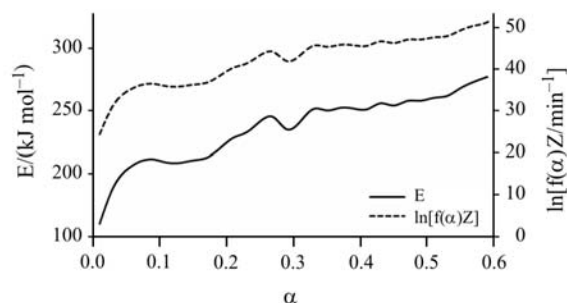


Fig. 11 BTAw (pre-dried at 50°C) IsoKin TG decomposition results for $\beta=1$ to $10^\circ\text{C min}^{-1}$

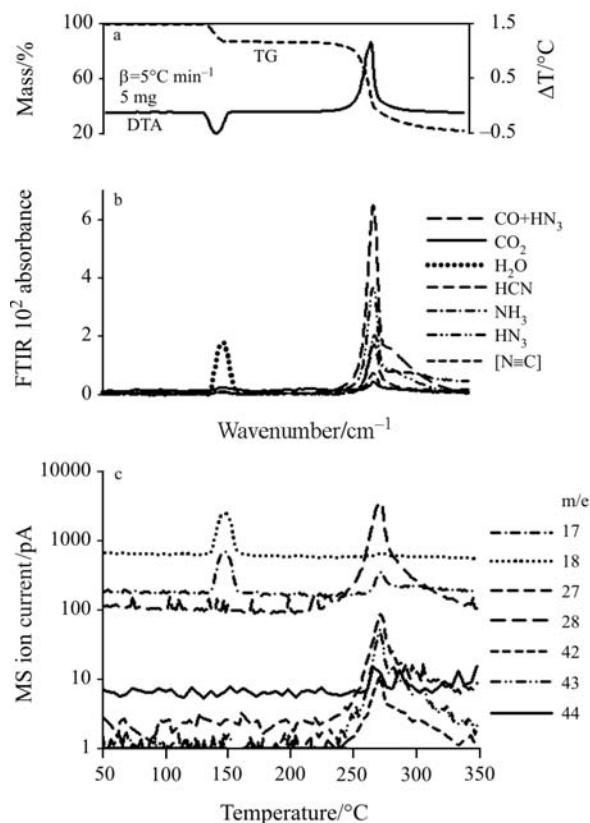


Fig. 12 5 mg BTaw heated in helium at 5°C min^{-1} : a – TG-DTA, b – FTIR and c – MS

plot for the thermal decomposition in helium is shown in Fig. 12. A 10–15% mass loss is observed in the 125 to 150°C range. This mass loss was attributed to dehydration, verified by the evolved gas analysis: the absorbance peak in the FTIR spectrum at 3854 cm^{-1} and the ion current peak for $m/e=18$ in the MS. A peak for the OH ion ($m/e=17$) was also present as a result of electron impact fragmentation of the water molecule. The mass of the water lost indicates that there is approximately 1 mol of water per mol of BTaw.

Hydrogen azide (2153 and 1165 cm^{-1}), ammonia (967 cm^{-1}) and hydrogen cyanide (714 cm^{-1}) appear as the major products in the FTIR trace in helium beginning at approximately 240°C . This is supported by the MS data with peaks appearing for $m/e=17$, 29 and 43. The second peak of $m/e=17$ was due to the evolution of ammonia, since no significant water ($m/e=18$) evolution was observed. A strong peak in the MS for $m/e=28$ could be due to CO and N_2 formed either by electron impact fragmentation of HN_3 , or by the thermal decomposition of BTaw. The total mass loss for this decomposition slowly approaches 80% by 350°C .

A TG-DTA-FTIR-MS plot for the thermal decomposition of BTaw in air is shown in Fig. 13. The same dehydration process is seen in the 125 to 150°C range. However, at approximately 262°C ,

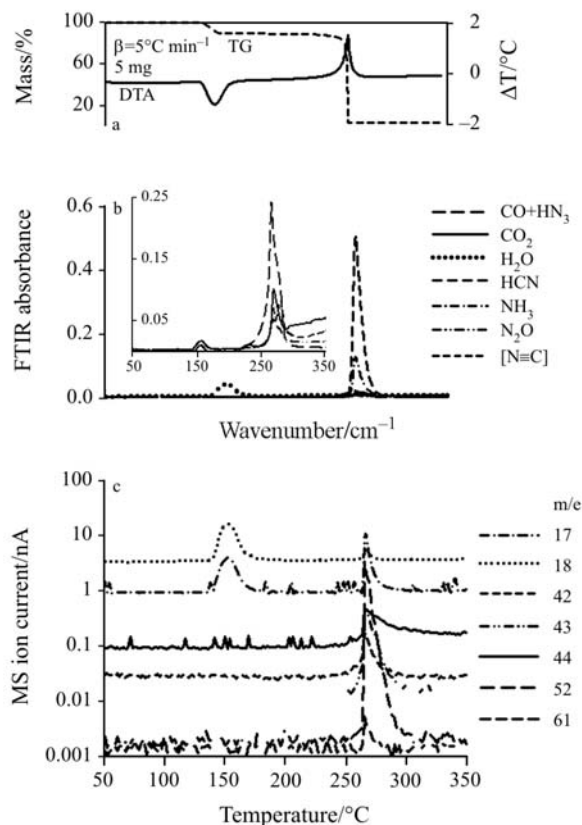


Fig. 13 5 mg BTaw heated in air at 5°C min^{-1} : a – TG-DTA, b – FTIR and c – MS

a sharp mass loss totalling almost 100% was observed. This was accompanied by the evolution of mainly hydrogen cyanide and ammonia, as well as small amounts of carbon monoxide, carbon dioxide and various other gases for which the identification is inconclusive.

FTIR absorbance in the 2280 to 2285 cm^{-1} region suggests the evolution of a nitrile compound in both He and air. The presence of $m/e=42$ suggests this nitrile may be cyanamide, however further work is needed for a definitive identification. The peak of $m/e=42$ can also be a fragment of HN_3 . However, a comparison of the intensities for $m/e=42$ and 43 suggests that $m/e=42$ is unlikely to only result from HN_3 . Nitrogen gas is thought to be evolved based on previous studies of the thermal decomposition of 5-aminotetrazole done by Levchik *et al.* [15]. However, there is no supporting evidence at this time due to the presence of nitrogen in the purge gas.

Tetrazole and 5-aminotetrazole both exhibit tautomerism, which is known to affect the mechanism of their thermal decomposition. When the thermal decomposition of tetrazole occurs in a melt, nitrogen is evolved as a result of breakdown of the azido-form of the molecule and approximately 5% of the sample decomposes with the elimination of hydrogen azide from the ring form of the molecule [16, 17]. With 5-aminotetrazole, fragmentation of the imino

form, the main isomer of the molecule in the solid state, most likely gives HN_3 [15, 18]. However, upon heating the imino form converts to the amino form and decomposition results in the elimination of nitrogen gas and ammonia. Using these two molecules for comparison, BTAw may undergo a tautomeric isomerization in which one form of the molecule has one or both tetrazole rings in an imino form and results in the elimination of hydrogen azide.

ARC results

The thermal behaviour of BTAw and BTA using ARC was studied in atmospheres of air and argon at ambient pressure. Figure 14 is an example of the results for a typical ARC experiment, showing temperature and pressure vs. time. A comparison of $\ln[R/(\text{°C min}^{-1} \text{g}^{-1})]$ vs. reciprocal temperature for the various methods used is shown in Fig. 15. Table 2

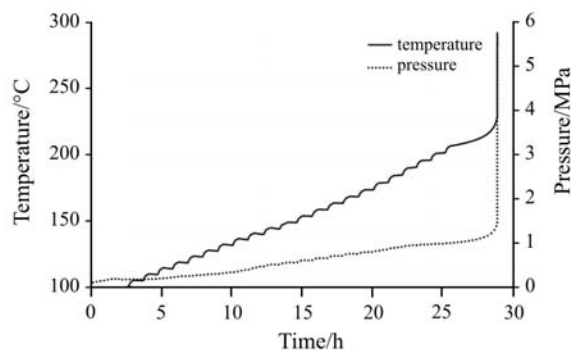


Fig. 14 Example of ARC results for BTAw: pre-dried at 50°C, and run in a closed system of ambient argon

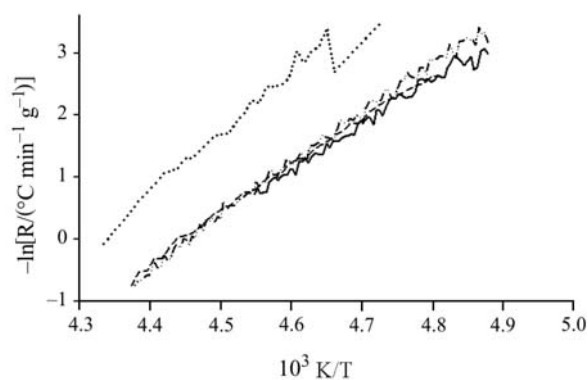


Fig. 15 Comparison of rate vs. temperature for various methods. Dried in situ at 120°C and then run in \cdots ambient air, pre-dried externally at 50°C and then run in $---$ ambient argon, pre-dried externally at 50°C and then run in $—$ ambient air, pre-dried externally at 120°C and then run in $- \cdots -$ ambient argon

presents a summary of the ARC results using the various drying methods.

BTAw samples were dried in situ at 120 °C followed by a HWS performed in an ambient air atmosphere using an initial temperature of 150°C. In this set of experiments, each reaction concluded with an exothermic reaction with a self-heating rate greater than the set maximum rate of 1°C min^{-1} . The experiments displayed consistent results, having onset temperatures of 213 and $215\pm 5\text{°C}$ and each ending in a runaway reaction.

In addition, samples of BTAw were dried externally at 50°C. HWS experiments were performed on these samples in both ambient argon and air. The re-

Table 2 Comparison of ARC results from the various drying methods

Drying method	Atmosphere	Sample mass/g	$T_i/\text{°C}$	$(T_o \pm 5)/\text{°C}^a$	P_f/MPa^b	$E/(\text{kJ mol}^{-1})$	$\ln(Z/\text{min}^{-1})$	$\ln(k/\text{min}^{-1})^c$
In situ at 120°C	air	0.48	150	213	0.37 at 20°C	418±7	100±2	-2±3
		0.49	150	215	0.30 at 22°C	425±10	101±2	-3±3
Externally at 50°C	argon	0.53	100	205	0.27 at 38°C	322±3	77.2±0.7	-1±1
		0.53	100	203	0.68 at 21°C	319±3	76.2±0.7	-2±1
Externally at 50°C	air	0.51	100	211	0.52 at 20°C	365±3	87.2±0.7	-2±1
		0.49	100	201	0.51 at 26°C	315±4	75±1	-2±1
Externally at 120°C	argon	0.50	100	203	0.48 at 25°C	351±2	84±5	-2±5
		0.50	100	198	0.53 at 39°C	326±2	78.1±0.6	-1.4±0.8

^auncertainty from the extrapolation of the onset temperature, ^bpressure recorded at ambient temperature following the run, ^c $\ln k$ calculated at 220°C

sults in argon exhibited similar behaviour with onset temperatures of 205 and 203±5°C. These runs also showed some unusual behaviour in which the heating rate attained the pre-determined self-heating rate limit, 1°C min⁻¹, which triggered cooling of the ARC, but after cooling had begun, the heating rates were in excess of 10°C min⁻¹ for a short time before cooling resumed. Similar experiments in ambient air did not exhibit this unusual behaviour and the onset temperatures for these experiments were 211 and 201±5°C. In spite of the potential oxidizing potential in air, there is no apparent difference between the onset temperatures for the ARC experiments conducted in inert gas or air.

Finally, HWS runs in ambient argon were carried out on samples of BTAW that were pre-dried at 120°C. This method of pre-drying removed all water content and resulted in BTA (verified by conducting a TG study on the sample). Onset temperatures of 198 and 203±5°C were observed, which are similar to, but slightly lower than, the previous experiments conducted in argon on a sample pre-dried at 50°C, suggesting that BTA is less thermally stable than BTAW. In addition, when comparing this sample to the sample dried *in situ* at 120°C, a significant decrease was seen in the onset temperature. This indicated that an increase in drying time – approximately 16 h for the external drying compared to 3 h for *in situ* drying – results in a decrease in the thermal stability and thus, the onset temperature.

From Fig. 15, it is apparent that all the experiments demonstrate similar variation of *R* with reciprocal temperature, with the exception of the sample dried *in situ*. For this sample, the onset temperature is slightly higher and the values of *R* are significantly larger than the other experiments throughout the entire temperature range. It should be noted that the initial temperature was also higher for this sample and this may have had an effect on these observations.

Conclusions

A DSC heating rate study was performed on the dehydration and decomposition of BTAW using the rates of 0.5, 1, 2 and 5°C min⁻¹. For the dehydration step, an activation energy of 197±5 kJ mol⁻¹ and a ln(*Z*/min⁻¹) value of 46±1 were obtained. For the decomposition step, values of 222±16 kJ mol⁻¹ and 38±4 min⁻¹ were calculated for the activation energy and the pre-exponential factor, respectively. The results from the half-life test indicated that the ASTM method E698 [4] provided a good estimate of the kinetic parameters for BTAW.

A second heating rate study, this time using TG, was performed on BTAW using 1, 2, 5 and

10°C min⁻¹. This yielded an activation energy of 236±5 kJ mol⁻¹ and a ln(*Z*/min⁻¹) value of 41±1. These results, in conjunction with the DSC results, provide a good estimate of the kinetic parameters for decomposition of BTA.

Results from DSC, TG, TG-DTA-FTIR-MS and ARC all suggest that BTAW first loses water before undergoing any exothermic reaction and that BTAW is more thermally stable than BTA. The enthalpy for the dehydration step is consistent with the energy of strong hydrogen bonding. Results from TG-DTA-FTIR-MS experiments indicate that BTAW decomposes with similar gaseous products as those from tetrazole and 5-aminotetrazole, which may suggest a similar mechanism of decomposition is involved. However, further studies are required, including an analysis of the solid residue left over after decomposition.

References

- 1 D. E. Chavez and M. A. Hiskey, *J. Pyrotechnics*, 7 (1998) 11.
- 2 D. E. Chavez, M. A. Hiskey and D. L. Naud, *J. Pyrotechnics*, 10 (1999) 17.
- 3 V. V. Nedelko, B. L. Korsounskii, A. V. Shastin, N. V. Chukanov and T. S. Larikova, in: *Proceedings of the 29th Annual Conference of ICT on Energetic Materials and Technology*, Karlsruhe, Germany, 30 June–3 July 1998.
- 4 ASTM E698–01, Standard Test Method for Arrhenius Kinetic Constants for Thermally Unstable Materials, American Society for Testing and Materials, West Conshohocken, PA, USA.
- 5 ASTM E968, Standard Practice for Heat Flow Calibration of Differential Scanning Calorimeters, American Society for Testing and Materials, West Conshohocken, PA, USA.
- 6 ASTM E967, Standard Practice for Temperature Calibration of Differential Scanning Calorimeters and Differential Thermal Analyzers, American Society for Testing and Materials, West Conshohocken, PA, USA.
- 7 ASTM E1582–00, Standard Practice for Calibration of Temperature Scale for Thermogravimetry, American Society for Testing and Materials, West Conshohocken, PA, USA.
- 8 R. Turcotte, R. C. Fouchard, A.-M. Turcotte and D. E. G. Jones, *J. Therm. Anal. Cal.*, 73 (2003) 105.
- 9 D. I. Townsend and J. C. Tou, *Thermochim. Acta*, 37 (1980) 1.
- 10 ASTM E1981-98, Standard Guide for Assessing the Thermal Stability of Materials by Methods of Accelerating Rate Calorimetry, American Society for Testing and Materials, West Conshohocken, PA, USA.
- 11 W. J. Moore, *Physical Chemistry*, 5th Edition, Longmans, London 1972, p. 728.
- 12 ASTM E1641–04, Standard Test Method for Decomposition Kinetics by Thermogravimetry, American Society for Testing and Materials, West Conshohocken, PA, USA.

- 13 C. A. Wight, Isoconversional Data Analysis Program, Center of Thermal Analysis, University of Utah, Version 1.42, 2000.
 - 14 S. Vyazovkin and D. Dollimore, *J. Chem. Inf. Comput. Sci.*, 39 (1996) 42.
 - 15 S. V. Levchik, O. A. Ivashkevich, A. I. Balabanovich, A. I. Lesnikovich, P. N. Gaponik and L. Costa, *Thermochim. Acta*, 207 (1992) 115.
 - 16 A. I. Lesnikovich, O. A. Ivashkevich, G. V. Printsev, P. N. Gaponik and S. V. Levchik, *Thermochim. Acta*, 171 (1990) 207.
 - 17 A. I. Lesnikovich, S. V. Levchik, A. I. Balabanovich, O. A. Ivashkevich and P. N. Gaponik, *Thermochim. Acta*, 200 (1992) 427.
 - 18 A. I. Lesnikovich, O. A. Ivashkevich, S. V. Levchik, A. I. Balabanovich, P. N. Gaponik and A. A. Kulak, *Thermochim. Acta*, 388 (2002) 233.
-
- CTAS 2005
OnlineFirst: October 20, 2006
-
- DOI: 10.1007/s10973-006-7719-7